RSC Advances

ROYAL SOCIETY OF CHEMISTRY

www.rsc.org/advances

Graphical Abstract

A new water soluble rhodamine-based dual 'off-on-off' probe that can selectively detect Hg(II) ions of low level in presence of large excess of competing ions and the resulting L-Hg complex is also an efficient sensor for sulfide anions in physiological conditions. This could be employed as a ratiometric fluorescence resonance energy transfer (FRET) based time dependent reversible chemosensor for imaging Hg(II) in living cells and whole bodies.

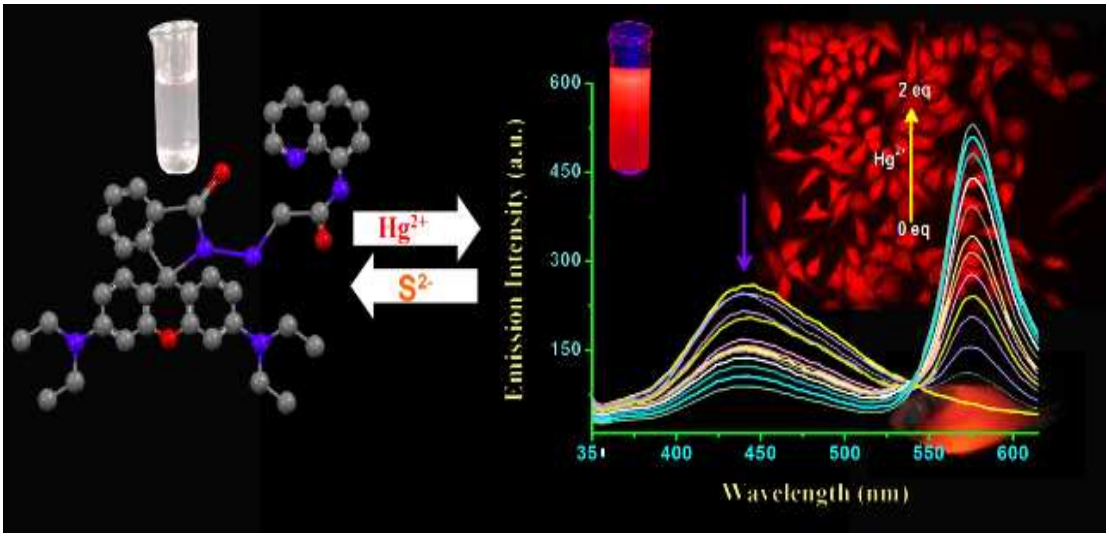

Cite this: DOI: 10.1039/c0xx00000x

www.rsc.org/xxxxxx

ARTICLE TYPE

A water soluble FRET-based ratiometric chemosensor for Hg(II) and S^{2-} applicable in living cell staining

Buddhadeb Sen,[a] Manjira Mukherjee,[a] Siddhartha Pal,[a] Koushik Dhara,[b] Sushil Kumar Mandal,[c] Anisur Rahman Khuda-Bukhsh,[c] and Pabitra Chattopadhyay*[,a]

Received (in XXX, XXX) Xth XXXXXXXXX 20XX, Accepted Xth XXXXXXXXX 20XX
DOI: 10.1039/b000000x

A new highly sensitive and selective Hg(II) probe, *2-(rhodamine-b-hydrazido)-N-(quinolin-8-yl)acetamide* (**L^1**) was developed and characterized. **L^1** specifically binds to Hg(II) in presence of large excess of other competing ions with visually observable changes in both electronic and fluorescence spectral behaviour to make possible significantly naked eye detection of Hg(II) of very low level (up to $4.5x10^{-7}$ M) through a fluorescence resonance energy transfer (FRET) process in HEPES buffer (1 mM, pH 7.4; 2% EtOH) at 25°C. The theoretical and experimental kinetic study also support the binding of Hg(II) ion to induce the opening of the spirolactam ring in **L^1** for enabling the FRET process. Further studies reveal that the dissociation of **L-Hg** complex in presence of sulphide anions selectively to restore the native structure of **L^1** is also useful in the detection of sulfide anions with a detection limit of submicromolar range in the same medium of HEPES buffer (1 mM, pH 7.4; 2% EtOH) at 25°C. **L^1** could be employed as a FRET based time dependent reversible chemosensor for imaging Hg(II) in living cells and whole bodies, and also be used as an imaging probe for the detection of uptake of sulfide ions in HeLa cells.

Introduction

Hg(II) is considered as one of the most hazardous and ubiquitous pollutants.[1] It is widely distributed in air, water, soil, and anthropogenic materials[2] through different processes such as volcanic emissions, mining, solid waste incineration, and the combustion of fossil fuels.[3] Inorganic mercury and its compounds can be accumulated in the body, and easily pass through biological membranes[4] such as skin, gastrointestinal and respiratory tissues and show a high affinity for thiol groups in proteins.[5] Very low levels of mercury ions is known to cause neurological, reproductive, cardiovascular, and developmental disorders, DNA damage, *Minamata disease*,[5] some kinds of autism and damage of the brain, kidneys, central nervous system, immune system and endocrine system.[4-6]

In general, several traditional methods[7] for the detection of mercury ions in various samples have been developed, including atomic absorption spectroscopy(AAS),[8] inductively coupled plasma mass spectroscopy (ICP-MS),[9] inductively coupled plasma-atomic emission spectrometry (ICP-AES),[10] capillary electrophoresis-ICP-MS[11] and high performance liquid chromatography-ICP-MS.[12] Although these methods are quantitative, most of these methods require expensive instruments and so these are not well-suited for quick in-field detection of Hg(II) or for *in vivo* studies of Hg(II) in biology and toxicology.

Fluorescence techniques have become powerful tools for sensing and imaging metal ions in trace amounts because of its simplicity, high sensitivity and real-time monitoring with a short response time.[13] Generally, Hg(II) ions are known to produce fluorescence quenching when binding to fluorophore molecules *via* the spin-orbit coupling effect. In consequence, the turn-off is the usual response upon binding in most instances. But the sensors with fluorescence enhancement (turn-on response) through Fluorescence Resonance Energy Transfer (FRET) are of considerable interest as FRET is a distance dependant radiationless transfer of energy from an excited donor fluorophore to a suitable acceptor fluorophore and it has been used to investigate molecular level interactions as it is sensitive to distance. However to date, a lot of rhodamine-based fluorescent probes for Hg(II) have been reported.[14-16] Among all these sensors, most of them performed in organic solvent or water with organic cosolvent,[15] only few of them work well in aqueous buffer solutions containing less than 20 % organic cosolvent.[16] As a result, there is an increasing demand to develop a rhodamine based probe for Hg(II) detection in a medium containing very less amount of organic cosolvent with a proper molecular level interaction through FRET.

Anion recognition and sensing has received considerable interest because of its pivotal role, play in the areas of biology, environmental hazards, medicine, catalysis, etc.[17] Among the anions, sulfide is one of the biologically and environmentally important anion as sulfide anions are generated not only as a byproduct in industrial processes but also in biosystems due to microbial reduction of sulfate by anaerobic bacteria and

formation of sulfur-containing amino acids in meat proteins.[18] Continuous exposure to sulfide anion can cause gradual and cumulative damage, such as loss of consciousness, irritation of mucous membranes, and suffocation.[19] Once protonated, it becomes HS^- or H_2S which are more toxic and caustic than the sulfide itself. However, recent studies have demonstrated that protonated sulfide can cause in reduction blood pressure, mediation of neurotransmission, inhibition of insulin signaling and regulation of inflammation.[20] In addition, H_2S levels are important in several diseases such as Alzheimer's disease,[21] Down's syndrome,[22] diabetes,[23] and liver cirrhosis.[24] Therefore, development of a quick and sensitive method for sulfide anion detection in aqueous media and in biological systems is very important for treatments and helpful toward understanding mechanism of action and regulation.

In this paper, we have designed and synthesized a new rhodamine-based chemosensor ($\mathbf{L^1}$) which behaves as a highly selective and ratiometric FRET-based fluorescent probe for Hg(II) in HEPES buffer (1 mM, pH 7.4; 2% EtOH) at 25°C. The fluorescence spectrum of $\mathbf{L^1}$ excited at 330 nm exhibits a fluorescence maximum at 440 nm which decreases along with the gradual increase of a new peak at 575 nm on addition of Hg(II). This phenomenon due to the ring-opening of the spirolactam system of rhodamine gives rise to strong fluorescence emission and also a visual color change from colorless to violet to pink. Ratiometric responses are more attractive because the ratio between the two emission intensities can be used to measure the analyte concentration and sensor molecule concentration, provide a built-in correction for environmental effects and stability under illumination.[13b,13c,25] Interestingly, the presence of an excess of the biologically relevant (Na^+, K^+, Ca^{2+} etc.) and other metal (Cr^{3+}, Mn^{2+}, Fe^{3+} etc.) ions does not affect the "switch ON" behaviour of the receptor $\mathbf{L^1}$ observed in presence of Hg(II) ions due to the formation of **L-Hg** complex which is reversible in nature. But the reversibility of the **L-Hg** system to regenerate $\mathbf{L^1}$ is only in the presence of S^{2-} anions and it results in "ON-OFF" behavior to sense sulphide anion in the same medium of HEPES buffer (1 mM, pH 7.4; 2% EtOH) at 25°C. The kinetics study of the reaction of Hg(II) with $\mathbf{L^1}$ showed two consecutive steps and it clearly indicated that the opening of spirolactam-ring was operated to produce xanthenes form after the chelation of $\mathbf{L^1}$ with Hg(II). Fluorescence microscopic studies confirmed that $\mathbf{L^1}$ could also be used as an imaging probe for detection of uptake of both ions in HeLa cells and whole bodies.

Experimental section

Materials and methods

High-purity HEPES, 8-aminoquinoline, 2-chloroacetyl chloride and mercury(II) nitrate monohydrate and mercury(II) chloride were purchased from Sigma Aldrich (India) and rhodamine B from E. Merck, Solvents used were spectroscopic grade. All metal salts were used as either their nitrate or their chloride salts. Other chemicals were of analytical reagent grade and used without further purification except when specified. Milli-Q, 18.2 MΩ cm^{-1} water was used throughout all experiments. A Shimadzu (model UV-1800) spectrophotometer was used for recording electronic spectra. FTIR spectra were recorded using Perkin Elmer FTIR model RX1 spectrometer preparing KBr disk. ^{1}HNMR spectrum of organic moiety was obtained on a Bruker Avance DPX 400 MHz spectrometer using DMSO-d_6 solution and for ^{13}C NMR it was 500MHz. Electrospray ionization (ESI) mass spectra were recorded on a Qtof Micro YA263 mass spectrometer. A Systronics digital pH meter (model 335) was used to measure the pH of the solution and the adjustment of pH were done using either 50 mM HCl or NaOH solution. Steady-state fluorescence emission and excitation spectra were recorded with a Perkin Elmer LS 55 spectrofluorimeter. Time-resolved fluorescence lifetime measurements were performed using a HORIBA JOBIN Yvon picosecond pulsed diode laser-based time-correlated single-photon counting (TCSPC) spectrometer from IBH (UK) at λ_{ex}= 340 nm and MCP-PMT as a detector. Emission from the sample was collected at a right angle to the direction of the excitation beam maintaining magic angle polarization (54.71). The full width at half-maximum (FWHM) of the instrument response function was 250 ps, and the resolution was 28.6 ps per channel. Data were fitted to multiexponential functions after deconvolution of the instrument response function by an iterative reconvolution technique using IBH DAS 6.2 data analysis software in which reduced w2 and weighted residuals serve as parameters for goodness of fit.

Synthesis of the probe ($\mathbf{L^1}$)

The probe $\mathbf{L^1}$ was synthesised by a 3 step reaction (Scheme-1).

At first, the rhodamine B-hydrazide (**1**) was prepared following a literature method.[26] In brief, 85% hydrazine hydrate (4 mL) was added to a solution of rhodamine B (1 g, 2.09 mmol) in ethanol (40 mL). The solution was refluxed for 6 h. Then, the reaction mixture was evaporated under reduced pressure to give an orange oil, which was then recrystallized from methanol-water to afford rhodamine B-hydrazide as a light-orange crystal (77%).

Then 2-chloro-N-(quinol-8-yl)acetamide (**2**) was prepared from the reaction of 2-chloroacetyl chloride and 8-aminoquinoline as follows-

2-Chloroacetyl chloride (5.31 mL) was dissolved in chloroform (5 mL) and then added dropwise to a cooled stirred solution of 8-aminoquinoline (2.88 g, 20 mmol) and Et_3N (3.0 mL) in chloroform (10 mL) within 1 h. After being stirred for 2 h at room temperature, the mixture was removed under reduced pressure to obtain a white solid, which was filtered out and extracted with dichloromethane to afford compound **2**.[27] Yield: 82 %. mp (°C): 133 ± 2.

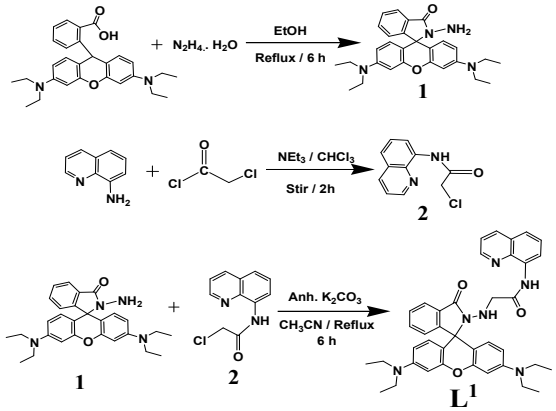

Scheme 1 Synthesis of $\mathbf{L^1}$

In the final step, rhodamine B-hydrazide (**1**) was taken in dry acetonitrile having anhydrous K_2CO_3 and 2-chloro-N-(quinolin-8-yl)acetamide (**2**) in dry acetonitrile was added dropwise at stirring condition. The resulting reaction mixture was refluxed for 6 h. The volume of the solution was reduced to obtain a solid and then extracted with dichloromethane and finally purified by silica gel column chromatography using dichloromethane as the eluent. Yield: 70 %, mp (^oC): 152 ± 2; Anal. Found: C, 73.54; H, 6.76; N, 12.89; Calc.: C, 73.10; H, 6.29; N, 13.12. IR (cm^{-1}): $\nu_{NH,}$ 3327; $\nu_{C=C,}$ 2971; $\nu_{C=O,}$ 1693; $\nu_{C=N,}$ 1614; ^{1}H NMR (400 MHz, DMSO-d6): 8.93 (dd, 1H), 8.59 (d, 1H), 8.41 (dd, 1H), 7.78-7.71 (m, 2H), 7.66-7.58 (m, 2H), 7.52-7.46 (m, 2H), 6.99-6.94 (m, 1H), 6.42-6.30 (m, 6H), 4.56 (s, 2H, -CH_2-CO), 3.29 (q, 8H, 4CH_2), 1.06 (t, 12H, 4CH_3); ^{13}C NMR (125 MHz, DMSO-d6): 165.22, 164.92, 152.98, 152.61, 151.89, 149.13, 148.13, 138.07, 136.66, 133.66, 132.34, 129.56, 128.08, 127.82, 127.65, 126.89, 123.44, 122.65, 122.28, 122.12, 116.59, 107.85, 105.50, 97.43, 64.72, 43.61, 12.38; ESI-MS m/z 640.99 [M+H^+, 10%], 663.00 [M+Na^+, 23%].

Synthesis of L-Hg Complex as [Hg(L)Cl_2]

To a 10 mL ethanol solution of $\mathbf{L^1}$ (0.01mmol), a solution of mercury(II) chloride was added dropwise and stirred for 4 h. Solvent was removed using a rotary evaporator, while a blood red solid was obtained (Scheme-S1). [Hg(L)Cl_2]: $C_{39}H_{40}Cl_2HgN_6O_3$: Anal. Found: C, 52.17; H, 4.30; N, 9.09; Calc.: C, 51.35; H, 4.42; N, 9.21. IR (cm^{-1}): $\nu_{NH,}$ 3295; $\nu_{C=C,}$ 2972; $\nu_{C=O,}$ 1686; $\nu_{C=N,}$ 1612; ^{1}H NMR (400 MHz, DMSO-d_6): 8.95 (dd, 1H), 8.62 (d, 1H), 8.44 (dd, 1H), 7.78-7.72 (m, 2H), 7.67-7.59 (m, 2H), 7.50-7.46 (m, 2H), 6.99-6.95 (m, 1H), 6.42-6.30 (m, 6H), 4.58 (s, 2H, -CH_2-CO), 3.31 (q, 8H, 4CH_2), 1.06 (t, 12H, 4CH_3) ESI-MS in methanol: $[M+Na]^+$, m/z, 935.11 (obsd. with 24 % abundance) (Calc.: m/z, 935.22; where M = [Hg(L)Cl_2]; Yield : 67-70%.

Emission study

Organic moiety ($\mathbf{L^1}$) shows a very weak emission at 575 nm in HEPES buffer (1 mM, pH 7.4; 2% EtOH) at 25°C when excited at 550 nm considering the absorption at 550 nm. Fluorescence quantum yields (Φ) were estimated by integrating the area under the fluorescence curves with the equation:

$$\Phi_{sample} = \Phi_{ref} X \frac{OD_{ref} \times A_{sample} \times \eta^2_{sample}}{OD_{sample} \times A_{ref} \times \eta^2_{ref}}$$

where A is the area under the fluorescence spectral curve and OD is optical density of the compound at the excitation wavelength, 550 nm, η is the refractive index of the solvent used. The standard used for the measurement of fluorescence quantum yield was rhodamine-B (Φ = 0.7 in ethanol).

General method of UV-vis and fluorescence titration

Path length of the cells used for absorption and emission studies was 1 cm. For UV-vis and fluorescence titrations, stock solution of $\mathbf{L^1}$ was prepared in HEPES buffer (1 mM, pH 7.4; 2% EtOH) at r.t. Working solutions of $\mathbf{L^1}$ and Hg(II) were prepared from their respective stock solutions. Fluorescence measurements were performed using 15 nm x 5 nm slit width. Except time dependent spectra, all the fluorescence and absorbance spectra were taken after 30 minutes of mixing of Hg(II) and $\mathbf{L^1}$ to acquire the optimised spectra.

Job's plot from fluorescence experiments and UV-vis

A series of solutions containing $\mathbf{L^1}$ and $Hg(NO_3)_2$ were prepared such that the total concentration of $\mathbf{L^1}$ remain constant in all the sets. The mole fraction (X) of Hg(II) ions was varied from 0.1 to 0.75. The absorbance at 555 nm was plotted against the mole fraction of Hg(II) ions in solution and also fluorescence intensity at 575nm was plotted against mole fraction of Hg(II) ions.

Calculation of Förster distance (R_0)

The Förster distance (R_0) for the FRET process was calculated from the following simplified equation below:[28,29]

$R_0 = 0.211\ [k^2 \eta^{-4} \Phi_D J_{DA}]^{1/6}$

$= 0.211\ [k^2 \eta^{-4} \Phi_D \int_0^\infty I_D(\lambda)\, \varepsilon_A(\lambda)\, \lambda^4\, d\lambda]^{1/6}$ (in Å)

Where η is the refractive index (η = 1.33 in water);[30] Φ_D is the quantum yield of the donor; k denotes the average squared orientational part of a dipole-dipole interaction, typically k^2 =2/3;[26] J_{DA} expresses the degree of spectral overlap between the donor emission and the acceptor absorption; $I_D(\lambda)$ is the normalized fluorescence spectra of the donor; $\varepsilon_A(\lambda)$ is the molar absorption coefficient of the acceptor.

Theoretical Calculation

To clarify the understanding of the configurations and the mechanism of process of enhancement of fluorescence, DFT calculations of the excited state character of the probes $\mathbf{L^1}$ and its corresponding **L-Hg** complexes were performed using Gaussian-09 software over a Red Hat Linux IBM cluster. Molecular level interactions have also been studied using density functional theory (DFT) with the B3LYP/6-31G (d) functional model and basis set.

Kinetic measurements

The kinetic studies were done on a Shimadzu UV 1601 PC spectrophotometer attached to a thermoelectric cell temperature controller (Model TCC 240A, accuracy ±0.1 °C. The absorption due to ligand was subtracted by using equi-molar ratio of ligand-HEPES buffer (1 mM, pH 7.4; 2% EtOH) mixture in the reference cell. The progress of the reaction was followed by monitoring the increase in absorbance at 550 nm. Conventional mixing technique was followed and pseudo first order conditions with respect to probe concentration, were maintained throughout the course of the reaction.

Preparation of cell and *in vitro* cellular imaging with $\mathbf{L^1}$

Human cervical cancer cell, HeLa cell line was purchased from National Center for Cell Science (NCCS), Pune, India and was used throughout the study. Cells were cultured in Dulbecco's modified Eagle's medium (DMEM, Gibco BRL) supplemented with 10% FBS (Gibco BRL), and 1% antibiotic mixture containing penicillin, streptomycin and neomycin (PSN, Gibco BRL), at 37°C in a humidified incubator with 5% CO_2. For experimental study, cells were grown to 80-90 % confluence, harvested with 0.025 % trypsin (Gibco BRL) and 0.52 mM EDTA (Gibco BRL) in PBS (phosphate-buffered saline, Sigma Diagnostics) and plated at desire cell concentration and allowed to re-equilibrate for 24 h before any treatment. Cells were rinsed with PBS and incubated with DMEM-containing $\mathbf{L^1}$ (10 μM, 1%

DMSO) for 30 min at 25°C. All experiments were conducted in DMEM containing 10% FBS and 1% PSN antibiotic. The imaging system was composed of a fluorescence microscope (ZEISS Axioskop 2 plus) with an objective lens [10×].

To find out the applicability of this sensor ($\mathbf{L^1}$) for visual detection of mercury in fish, an experiment was carried out with *Chanda Nama* fish. The fishes were treated with aqueous Hg(II) (10 μM) for 30 min, washed with PBS to remove any Hg^{2+} adhering to the surface, and were subsequently treated with a solution of $\mathbf{L^1}$ (10 μM in DMSO) for 20 min, washed with PBS. The visual images were taken with a digital camera.

Cell Cytotoxicity Assay

To test the cytotoxicity of $\mathbf{L^1}$, MTT [3-(4,5-dimethyl-thiazol-2-yl)-2,S-diphenyl tetrazolium bromide] assay was performed by the procedure described earlier.[31] After treatments of the probe (5, 10, 20, 50, and 100 μM), 10μl of MTT solution (10 mg/ml PBS) was added in each well of a 96-well culture plate and incubated continuously at 25°C for 6 h. All mediums were removed from wells and replaced with 100μl of acidic isopropanol. The intracellular formazan crystals (blue-violet) formed were solubilized with 0.04 N acidic isopropanol and the absorbance of the solution was measured at 595 nm wavelength with a microplate reader. Values are means ± S.D. of three independent experiments. The cell cytotoxicity was calculated as percent cell cytotoxicity = 100% cell viability.

Result and discussion

Synthesis and characterisation

The synthesis of $\mathbf{L^1}$ involves first the conversion of rhodamine B to rhodamine B-hydrazide and then 2-chloro-*N*-(quinolin-8-yl)acetamide was prepared from the reaction of 2-chloroacetyl chloride and 8-aminoquinoline in chloroform medium in presence of NEt_3 (Scheme 1). Then the probe, $\mathbf{L^1}$ was isolated from the reaction of rhodamine B-hydrazide and 2-chloro-*N*-(quinolin-8-yl)acetamide in a dry acetonitrile solution in presence of anhydrous K_2CO_3. The formulation of $\mathbf{L^1}$ was confirmed by physico-chemico and spectroscopic methods (Fig. S1A-S1G†).

UV-vis Spectroscopic Studies of $\mathbf{L^1}$ in Presence of Hg(II)

UV-vis spectra of $\mathbf{L^1}$ was recorded in HEPES buffer (1 mM, pH 7.4; 2% EtOH) at 25°C shows an absorption maximum at 314 nm which may possibly be attributed to the intramolecular π-π* charge transfer (CT) transition. The absorption intensity of $\mathbf{L^1}$ at 314 nm gradually increased, accompanied by the formation of a new absorption peak at 555 nm (Fig. 1) as the Hg(II) was increased stepwise (0-30 μM) and the solution turned from colorless to pink (Fig. S2†).

The absorption value at 555 nm were gradually enhanced when the added concentrations of Hg(II) to $\mathbf{L^1}$ were increased from 0 to 30 μM, respectively which is concomitant to the visual color change of the solution from colorless to pink via an intermediate colour change blue violet with time (Fig. 2).

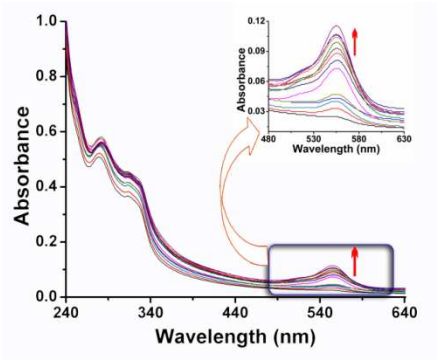

Fig. 1 UV-vis titration spectra of $\mathbf{L^1}$ (10 μM) upon incremental addition of Hg(II) (0-30 μM) in HEPES buffer (1 mM, pH 7.4; 2% EtOH) at 25°C.

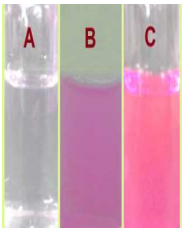

Fig. 2 Naked eye color change with time, (A) only probe, (B) immediately and (C) 30 min after addition of Hg(II) ion in HEPES buffer (1 mM, pH 7.4; 2% EtOH) at 25°C.

On account of the complexity of the intracellular environment, an additional examination of the probe was performed to determine whether other ions were potential interferents or not. To establish this fact, metal ion selectivity assays were performed while keeping the other experimental condition unchanged. No significant change in the UV-vis spectral pattern was observed upon the addition of 10 equivalents excess of relevant metal ions *i.e.* Na(I), K(I), Ca(II), Mg(II), Al(III), Cr(III), Mn(II), Fe(III), Co(II), Ni(II), Zn(II), Cd(II), and Pb(II).

Fluorescence Spectroscopic Studies of $\mathbf{L^1}$ in Presence of Hg(II)

In absence of Hg(II) ion, $\mathbf{L^1}$ exhibited fluorescence of weak intensity and showed pH independency over the pH range 6.0 to 10.0 (Fig. S3†). The emission spectrum of the $\mathbf{L^1}$ excited at 330 nm exhibits a fluorescence maximum at 440 nm in HEPES buffer (1 mM, pH 7.4; 2% EtOH) at 25°C. The intensities at 440 nm were significantly decreased with a concomitant increase in intensities at 575 nm showing an isoemissive point at near about 540 nm, when various concentrations of Hg(II) (0-30 μM) were added (Fig. 3).

Ratiometric signaling of fluorescence output at two different wavelengths plotted as a function of concentration of Hg(II) indicates that the fluorescence intensity ratio of wave length 440 nm and 575 nm (I_{575}/I_{440}) gradually increases with increase of the concentration of Hg(II) ions (*viz.* Fig. 3).

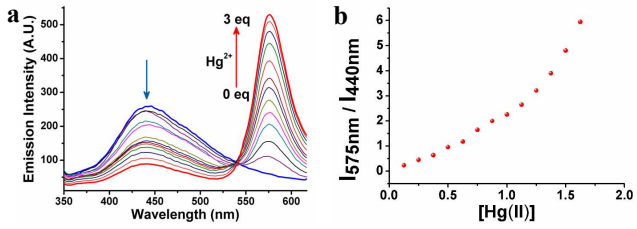

Fig. 3 (a) Emission spectra of $\mathbf{L^1}$ in presence of Hg(II) (0-30 μM) at λ_{ex} = 330 nm in HEPES buffer (1 mM, pH 7.4; 2% EtOH) at 25°C. (b) Ratiometric signaling of fluroscence output at two different wavelengths is plotted as a function of concentration of Hg(II) in HEPES buffer (1 mM, pH 7.4; 2% EtOH) at 25°C.

$\mathbf{L^1}$ exhibited a near about 45-fold increase of its fluorescence intensity upon addition of only 3.0 equivalent of Hg(II) ion. The detection limit was determined and was found to be 90 ppb (Fig. S4†), which is significantly low. Interestingly, the introduction of other metal ions causes the fluorescence intensity to be either unchanged or weakened. A metal ion selectivity study was then performed for $\mathbf{L^1}$ to understand this phenomenon under identical experimental conditions. Fluorescence enhancement of $\mathbf{L^1}$ (10 μM) was not observed upon addition of excess 50 equivalents of biologically relevant metal ions *i.e.* Na(I), K(I), Ca(II), and Mg(II) and 10 equivalents excess of several competitive metal ions [Al(III), Cr(III), Mn(II), Fe(III), Co(II), Ni(II), Cu(II), Zn(II), Cd(II), and Pb(II)] (Fig. S5†), and also in naked eye (Fig. S6 and S7†). In presence of 10 times excess of various tested ions together with $\mathbf{L^1}$ and Hg(II), almost no adverse effect on intensity was observed (Fig. S8†). Time dependent fluorescence spectrum also shows that the emission band at 440 nm diminishes with the appearance of an intense emission band at 575 nm (Fig. 4).

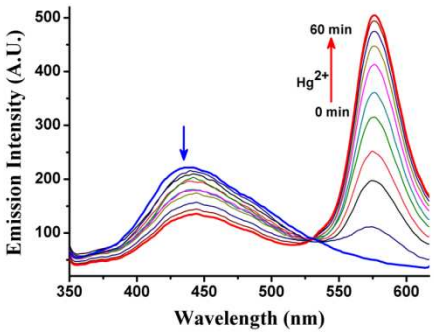

Fig. 4 Fluorimetric titration spectra of $\mathbf{L^1}$ (10μM) with Hg(II) (10μM) at λ_{ex} = 330nm with time in HEPES buffer (1 mM, pH 7.4; 2% EtOH) at 25°C.

As the receptor $\mathbf{L^1}$ bears two different fluorophore units, we consider it to be appropriate to study the metal binding event of $\mathbf{L^1}$ at two different excitation wavelengths corresponding to the excitation wavelength of the xanthene unit (550 nm) and quinoline unit (330 nm). Fig. 5 showed that excitation of $\mathbf{L^1}$ at 550 nm in absence of Hg(II) did not show any significant emission over the range from 550 to 700 nm initially with a quantum yield of only 0.03. This supports the facts that the receptor remains in the spirolactum form in absence of metal ions, and the nonexistence of the highly conjugated xanthene form results in the suppression of emission in the above mentioned region. But the addition of Hg(II) to this chemosensor ($\mathbf{L^1}$) induces a significant switch *ON* fluorescence response near 575 nm, with a visual display of reddish fluorescence.

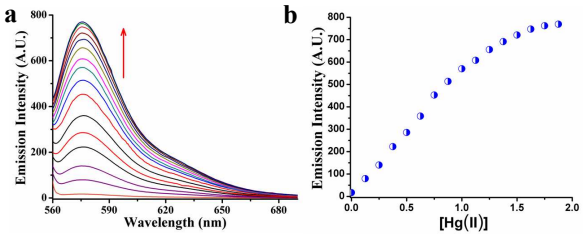

Fig.5 (a) Fluorimetric titration spectra of $\mathbf{L^1}$ with Hg(II) (0-30 μM) at λ_{ex} = 550nm in HEPES buffer (1 mM, pH 7.4; 2% EtOH) at 25°C, (b) Fluorescence intensity as a function of Hg(II) concentration at λ_{ex} = 550 nm in HEPES buffer (1 mM, pH 7.4; 2% EtOH) at 25°C.

Switch *ON* response for the absorption spectral band at 555 nm and the emission band at ~575 nm on binding to Hg(II) suggest the opening of the spirolactam ring of $\mathbf{L^1}$ on metal ion coordination (Scheme 2). It is observed that Hg binding with $\mathbf{L^1}$ to form **L-Hg** species induced ring-opening of $\mathbf{L^1}$ and the generation of xanthene moiety that is selective toward Hg(II) ion and does not reveal any noticeable spectral change for other tested metal ions together.

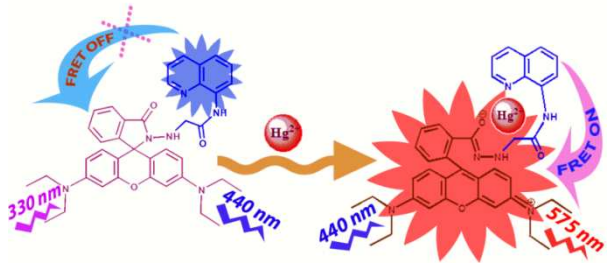

Scheme 2 Probable mechanism of Hg(II) induced FRET process.

The binding of Hg(II) ion induces opening of the spirolactam ring of $\mathbf{L^1}$ with an associated switch on UV-vis spectral response in the range 450-600 nm, which has a significant spectral overlap with the emission spectrum of the *N*-(quinol-8-yl)-acetamide fragment (Fig. S9†) and this fact unlocks a plausible route for nonradiative transfer of excitation energy from donor quinoline to acceptor xanthene moiety within Förster critical distance (R_0) which was calculated to be 40.6 Å, and initiates an intramolecular FRET process (*viz.* Scheme 2). In the free state of $\mathbf{L^1}$ the FRET pathway is totally suppressed, and only an emission maximum near 440 nm is observed when excited at 330 nm. Binding of the receptor to Hg(II) induces the FRET process to produce an intense rhodamine-based reddish emission; i.e., energy transfer from *N*-(quinol-8-yl)- acetamide moiety to xanthene is due to the ring-opening[32] resulting in increase of overlap integral between *N*-(quinol-8-yl)-acetamide and xanthene moiety. Thus, when titrated with increasing concentration of Hg(II) the emission band with a λ_{max} near 440 nm starts to decrease along with a concomitant generation of a new fluorescence band at 575 nm. This change in fluorescence was also observed visually, and the color changed to pink through violet (*viz.* Fig. 2).

The complex formed between $\mathbf{L^1}$ and Hg(II) is found to be 1:1

in stoichiometry, which is established with the help of Job's plot (Fig. S10 and S11 †) by the fluorescence and absorbance study also. The apparent binding constant (K) determined by the Benesi-Hilderbrand method[33] was estimated to be 6.73×10^6 M^{-1} (Fig. S12†). Further confirmation of 1:1 stoichiometry was obtained by the physico-chemical and spectroscopic data of the **L-Hg** complex isolated in the solid form and ^{1}H NMR titration is also in support of the chelation of $\mathbf{L^1}$ in solution state (Fig. S13†). The molecular-ion peak in ESI-MS of L-Hg was observed at m/z 935.11 evidenced to the 1:1 stoichiometric species (Fig. S1F†).

The proposed mechanism also resembles with the fluorescence lifetime data (Fig. 6, Tables 1 and 2). In the fluorescence life time experiment (λ_{em}= 440 nm), the average lifetime was found to be 1.75 ns. After 5 min of the addition of Hg(II) to the solution of $\mathbf{L^1}$, the average lifetime (λ_{em}= 440 nm) of the **L-Hg** species increased to 2.44 ns which is ascribed to the chelation enhanced fluorescence (CHEF) process. After 30 min, the value reduces to 1.11 ns, corresponds to the decrease of CHEF process of **L-Hg** system with time as proposed in the mechanism (Scheme 2). On the contrary, the average lifetime of **L-Hg** system after 30 min (λ_{em}= 575 nm) was increases from 1.72 ns to 2.10 ns, that resembles with the Hg(II)-induced FRET process, (*viz.* Fig. 6).

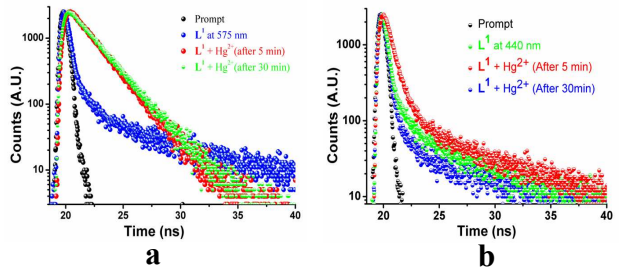

Fig. 6 Time resolved fluorescence decay of $\mathbf{L^1}$ (10μM) only and in presence of added Hg(II) (10 μM) in HEPES buffer (1 mM, pH 7.4; 2% EtOH) at 25°C using a nano LED of 340 nm as the light source (a) at λ_{em} = 575 nm, (b) at λ_{em} = 440nm.

Table 1 Fluorescence life time (ns) of the corresponding singlet excited states of $\mathbf{L^1}$ and **L-Hg**.

System		τ_{av} (ns) at λ_{em}= 440 nm	χ^2	τ_{av} (ns) at λ_{em}= 575 nm	χ^2
L^1		1.75	1.13	1.72	1.07
	after 5 min	2.44	1.07	1.98	1.01
L-Hg complex	after 20 min	1.11	1.12	2.10	1.00

According to the equations:[34] $\tau^{-1} = k_r + k_{nr}$ and $k_r = \Phi_f/\tau$, where k_r=the radiative rate constant, and k_{nr}=total nonradiative rate constant, the values of k_r and k_{nr} for the organic moiety, $\mathbf{L^1}$ and **L-Hg** species were listed in Table 2. The data suggest that k_r has just slightly changed but the factor that induces fluorescent enhancement is mainly ascribed to the decrease of k_{nr}.

Table 2 Fluorescence quantum yield (Φ) and life time (ns) of $\mathbf{L^1}$ and L-Hg at λ_{em}= 575 nm.

λ_{em}= 575 nm	Φ	τ_{av} (ns)	k_r (10^8 s^{-1})	k_{nr} (10^9 s^{-1})	χ^2
$\mathbf{L^1}$	0.03	1.72	0.2	0.56	1.07
L-Hg	0.43	2.10	2.0	0.36	1.00

Kinetics study

To verify the sequence of the reaction of Hg(II) with the probe ($\mathbf{L^1}$) in terms of chelation and ring opening, an experiment was performed to get the plot of $\ln(A_\infty - A_t)$ (where A_∞ is the absorbance at infinite time, and A_t is absorbance at time t) against time (t) which is found to be nonlinear (Fig. S14†). This is curved at initial stage and subsequently of constant slope indicating that the reaction proceeds *via* two consecutive steps. The first step is dependent on [Hg(II)] and it is due to chelation. Using the Weyh and Hamm's method,[35] the rate constant (k_1) was calculated from the plot of lnΔ *versus* time (t) where time (t) is small. The second step is the ring opening step as it is independent of [Hg(II)]. At a particular temperature (40 °C) the slope of $\ln(A_\infty - A_t)$ *versus* time (t) plots for different [Hg(II)] were found constant in the linear region. From this limiting linear portion of the plot, k_2 values were obtained directly from the slope for different [Hg(II)]. The calculated values for k_1 and k_2 are tabulated in Table S1†.

The overall p*seudo* first-order kinetic plot of the reaction of $\mathbf{L^1}$ (10 μM) with Hg(II) ((0.1-1.0 mM)) in HEPES buffer (1 mM, pH 7.4; 2% EtOH) at 25 °C was also done from the fluorescence emission intensity, and from the slope the overall rate constant, k' was found to be 9.66×10^{-4} sec^{-1} (Fig. S15†).

Spectroscopic Studies of L-Hg Complex in Presence of S^{2-}

To gain an insight into the fact of reversibility of ring-opening of spirolactam form to the generation of xanthene form, the rupture of the **L-Hg** species to regenerate $\mathbf{L^1}$ and the subsequent change of optical properties of **L-Hg** system were also studied (Fig. 16†). This fact is in support of reclaim of $\mathbf{L^1}$ from **L-Hg** system in presence of S^{2-}. Here several anions (F^-, Cl^-, Br^-, I^-, CN^-, NO_3^-, ClO_4^-, $H_2PO_4^-$, HPO_4^{2-}, OAc^-, SO_4^{2-}, $S_2O_3^{2-}$, CrO_4^{2-}, S^{2-}, SCN^-, and PO_4^{3-}) were used but only S^{2-} selectively quenches the fluorescence intensity of **L-Hg** system (Fig. 7).

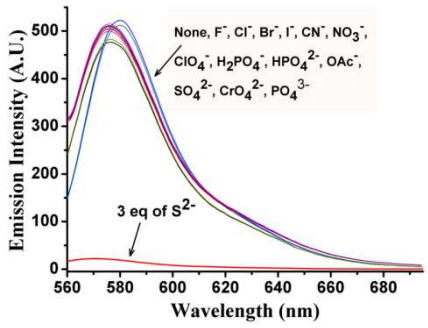

Fig. 7 Changes in the fluorescence spectra of **L-Hg** complex in presence of different anions (λ_{ex} = 550 nm).

This phenomenon proves that the regeneration of $\mathbf{L^1}$ was occurred selectively by the rupture of **L-Hg** species and simultaneous lowering of fluorescence intensity at 575 nm was observed and hence the fluorescence "*ON-OFF*" switching property of **L-Hg** complex could be used as ratiometric sensor for the detection of S^{2-} ion in physiological conditions (1 mM HEPES buffer, pH 7.4; 2% EtOH; at 25°C) (Fig. 8).

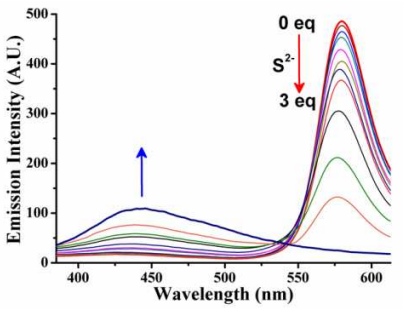

Fig. 8 Fluorescence titration spectra (λ_{ex} = 330 nm) of $\mathbf{L^1}$ (10 μM) with 2 equiv of Hg(II) upon continuous addition of sodium sulphide (up to 30 μM) in HEPES buffer (1 mM, pH 7.4; 2% EtOH) at 25°C.

The LOD value for sulphide ion in this method was found to be $1.7x10^{-7}$ M (Fig. S17†). The intensities of the fluorescence were recorded within 30 min after sulfide anion addition and it was varied with time. As a result of this fact it may be concluded that the monitoring system is virtually real-time and stable, and the sensor $\mathbf{L^1}$ was recycled during the detection of sulfide anions.

Theoretical Study

From theoretical calculation it is reflected that the HOMO and LUMO of $\mathbf{L^1}$ are less stabilized than **L-Hg** complex (Fig. 9). From the energy optimization of HOMO and LUMO of **L-Hg** complex, it could be easily pointed out that the more electronic charge density in HOMO over the rhodamine unit is pulled towards the quinoline unit in the LUMO. The energy gap between HOMO and LUMO are less in case of free ligand i.e. spirolactum ring form than L-Hg complex i.e. xanthene form.

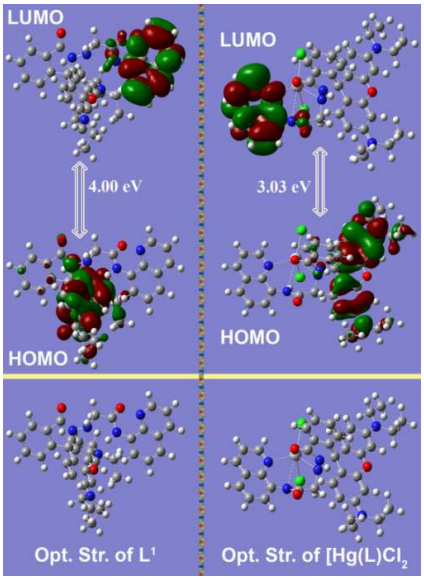

Fig. 9 Optimized structures of $\mathbf{L^1}$ and **L-Hg** complex.

Biological Studies of $\mathbf{L^1}$ in Presence of Hg(II) and S^{2-}

To examine the utility of the probe in biological systems, it was applied to human cervical cancer HeLa cell and *Chanda Nama* fish. In these experiments both the Hg(II) and $\mathbf{L^1}$ was allowed to uptake by the cells of interest and the images of the cells were recorded by the fluorescence microscopy following excitation at ~550 nm. After incubation with $\mathbf{L^1}$ (10 μM) for 30 min, the cells displayed very faint intracellular fluorescence. However, cells exhibited intensive fluorescence when exogenous Hg(II) was introduced into the cell via incubation with Hg-salt (Fig. 10). The fluorescence responses of the probe with various concentrations of added Hg(II) are clearly evident from the cellular imaging. Moreover, the intensive fluorescence was deeply suppressed by scavenging Hg(II) from the cell with the addition of Na_2S (Fig. 11). This experiment proves that the binding of Hg(II) with this chemosensor, $\mathbf{L^1}$, is readily reversible inside the cellular environment. In addition, the *in vitro* study showed that 10 μM of $\mathbf{L^1}$ did not show no cytotoxic effect to cell upto 6 h (Fig. S18†). These results indicate that the probe has a huge potentiality for both *in vitro* and *in vivo* application as Hg(II) sensor as well as imaging in different ways as same manner for live cell imaging can be followed instead of fixed cells.

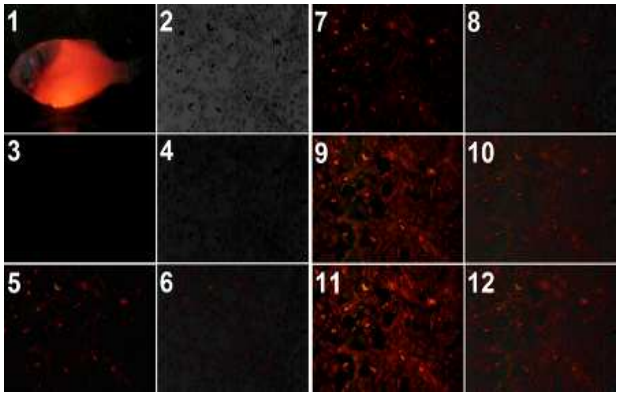

Fig. 10 (1) Fish; (2) Phase contrast; fluorescence, and ratio image of HeLa cells after incubation with (3, 4) 0 μM; (5, 6) 3 μM; (7, 8) 5 μM; (9, 10) 8 μM; (11, 12) 10 μM Hg(II) with $\mathbf{L^1}$ for 30 min at 25°C respectively and the samples were excited at ~550 nm.

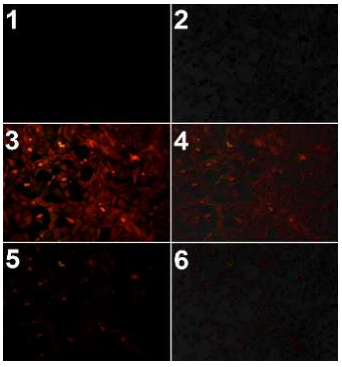

Fig. 11 Fluorescence, and its corresponding ratio image of HeLa cells after incubation with (1, 2) 0 μM, (3, 4) 10 μM with Hg(II) and (5, 6) 15 μM of Na_2S with $\mathbf{L^1}$ respectively for 30 min at 25°C and the samples were excited at λ= 550 nm.

Conclusions

In summary, we may conclude that a newly designed fluorescent chemosensor ($\mathbf{L^1}$) behaves as a highly specific and selective FRET-based ratiometric fluorescence probe towards Hg(II) that can also be detected by naked eye. On excitation at 330 nm the fluorescence spectrum of this probe exhibits a fluorescence maximum at 440 nm by CHEF which decreases with the gradual increase of a new peak at 575 nm on addition of Hg(II) due to the ring-opening of the spirolactam system of rhodamine for FRET to enable this probe to act as a ratiometric sensor of greater advantages and this phenomenon also gives rise to a visual colour change from colourless to violet to pink. Dissociation of the **L-Hg** complex formed is taken place only in presence of sulfide anion, and this fact enables **L-Hg** complex to be an efficient sensor for sulfide anions. By the incubation of cultured living cells (HeLa) with $\mathbf{L^1}$, intracellular Hg(II) and S^{2-}could be monitored through fluorescence microscopy study.

Acknowledgments

Financial assistance from CSIR, New Delhi, India is gratefully acknowledged. B. Sen wishes to thank to UGC, New Delhi, India for offering him the fellowship. We sincerely acknowledge Prof. Samita Basu and Mr. Ajay Das, Chemical Science Division, SINP, Kolkata for enabling TCSPC instrument.

Notes and references

[a] *Department of Chemistry, The University of Burdwan, Golapbag, Burdwan 713104, India. E-mail: pabitracc@yahoo.com*
[b] *Department of Chemistry, Sambhu Nath College, Labpur, Birbhum 731303, W.B, India.*
[c] *Molecular Biology and Genetics Laboratory, Department of Zoology, Kalyani University, India*

† Electronic Supplementary Information (ESI) available: [Experimental section, tables, schemes, figures, characterization data, and some spectra], See DOI: 10.1039/b000000x/

‡ Footnotes should appear here. These might include comments relevant to but not central to the matter under discussion, limited experimental and spectral data, and crystallographic data.

Corresponding Author
* E-mail: pabitracc@yahoo.com. Tel: +91-342-2558554 extn. 424. Fax: +91-342-2530452.

1 (a) Q. Wang, D. Kim, D. D. Dionysiou, G. A. Sorial and D. Timberlake, *Environ. Pollut.*, 2004, **131**, 323; (b) H. H. Harris, I. J. Pickering and G. N. George, *Science*, 2003, **301**, 1203.
2 P. Grandjean, P. Weihe, R. F. White and F. Debes, *Environ. Res*., 1998, **77**, 165.
3 (a) R. Von Burg and M. R. Greenwood, *Metals and their Compounds in the Environment*, VCH, Weinheim, 1991, 1045; (b) A. Renzoni, F. Zino and E. Franchi, *Environ. Res.*, 1998, **77**, 68.
4 (a) X. Zhang, Y. Xiao and X. Qian, *Angew. Chem. Int. Ed.*, 2008, **47**, 8025; (b) G. Guzzi and C. A. M. La Porta, *Toxicology*, 2008, **244**, 1.
5 M. Harada, Crit. *Rev. Toxicol.*, 1995, **25**, 1.
6 (a) C. M. L. Carvalho, E. -H. Chew, S. I. Hashemy, J. Lu and A. Holmgren, *J. Biol. Chem*., 2008, **283**, 11913; (b) T. W. Clarkson, L. Magos and G. J. Myers, *New Engl. J. Med.*, 2003, **349**, 1731.
7 K. Leopold, M. Foulkes and P. Worsfold, *Anal. Chim. Acta*, 2010, **663**, 127.
8 (a) Y. Gao, Z. Shi, Z. Long, P. Wu, C. Zheng and X. Hou, *Microchem. J.*, 2012, **103**, 1; (b) A. Q. Shah, T. G. Kazi, J. A. Baig, H. I. Afridi and M. B. Arain, *Food Chem.*, 2012, **134**, 2345.
9 (a) E. Kenduzler, M. Ates, Z. Arslan, M. McHenry and P. B. Tchounwou, *Talanta*, 2012, **93**, 404; (b) F. Moreno, T. Garcia-Barrera and J. L. Gomez-Ariza, *Analyst*, 2010, **135**, 2700.
10 X. Chai,; X. Chang, Z. Hu, Q. He, Z. Tu and Z. Li, *Talanta*, 2010, **82**, 1791.
11 Y. Zhao, J. Zheng, L. Fang, Q. Lin, Y. Wu, Z. Xue and F. Fu, *Talanta*, 2012, **89,** 280.
12 (a) X. Jia, Y. Han, X. Liu, T. Duan and H. Chen, *Spectrochim. Acta Part B*, 2011, **66**, 88; (b) Y. Yin, M. Chen, J. Peng, J. Liu and G. Jiang, *Talanta*, 2010, **81**, 1788.
13 (a) S. Sen, T. Mukherjee, B. Chattopadhyay, A. Moirangthem, A. Basu, J. Marek and P. Chattopadhyay, *Analyst*, 2012, **137**, 3975; (b) S. Sen, S. Sarkar, B. Chattopadhyay, A. Moirangthem, A. Basu, K. Dhara and P. Chattopadhyay, *Analyst*, 2012, **137**, 3335; (c) S. Sen, T. Mukherjee, S. Sarkar, S. K. Mukhopadhyay and P. Chattopadhyay, *Analyst*, 2011, **136,** 4839; (d) U. C. Saha, K. Dhara, B. Chattopadhyay, S. K. Mandal, S. Mondal, S. Sen, M. Mukherjee, S. V. Smaalen and P. Chattopadhyay, *Org. Lett.*, 2011, **13**, 4510; (e) U. C. Saha, B. Chattopadhyay, K. Dhara, S. K. Mandal, S. Sarkar, A. R. Khuda-Bukhsh, M. Mukherjee, M. Helliwell and P. Chattopadhyay, *Inorg. Chem.*, 2011, **50**, 1213; (f) K. Dhara, U. C. Saha, A. Dan, M. Manassero, S. Sarkar and P. Chattopadhyay, *Chem. Commun*., 2010, **46**, 1754.
14 (a) C. Wang and K.M.-C. Wong, *Inorg. Chem*. 2013, **52**, 13432; (b) P. Mahato, S. Saha, E. Suresh, R. Di Liddo, P. P. Parnigotto, M. T. Conconi, M. K. Kesharwani, B. Ganguly and A. Das, *Inorg. Chem*., 2012, **51**, 1769; (c) H. N. Kim, S.-W. Nam, K. M. K. Swamy, Y. Jin, X. Q. Chen, Y. Kim, S.-J. Kim, S. Park and J. Yoon, *Analyst*, 2011, **136**, 1339; (d) M. Kumar, N. Kumar, V. Bhalla, H. Singh, P. R. Sharma and T. Kaur, *Org. Lett*., 2011, **13**, 1422; (e) K. M. K. Swamy, H. N. Kim, J. H. Soh, Y. Kim, S.-J. Kim and J. Yoon, *Chem. Commun*., 2009, 1234. (f) X. Zhang, Y. Xiao and X. H. Qian, *Angew. Chem., Int. Ed*., 2008, **47**, 8025; (g) Y. Shiraishi, S. Sumiya, Y. Kohno and T. Hirai, *J. Org. Chem*., 2008, **73**, 8571; (h) Y. K. Yang, K. J. Yook and J. Tae, *J. Am. Chem. Soc*., 2005, **127**, 16760.
15 (a) R. Pandey, R. K. Gupta, M. Shahid, B. Maiti, A. Misra and D. S. Pandey, *Inorg. Chem*., 2012, **51**, 298; (b) Q.-B. Mei, Y.-H. Guo, B.-H. Tong, J.-N. Weng, B. Zhang and W. Huang, *Analyst*, 2012, **137**, 5398; (c) A. Thakur, S. Sardar and S. Ghosh, *Inorg. Chem*., 2011, **50**, 7066; (d) D. Y. Liu, K. Z. Tang, W. S. Liu, C. Y. Su, X. H. Yan, M. Y. Tan and Y. Tang, *Dalton Trans*., 2010, **39**, 9763; (e) Y. Zhou, C.-Y. Zhu, X.-S. Gao, X.-Y. You and C. Yao, *Org. Lett*., 2010, **12**, 2566; (f) M. Suresh, A. K. Mandal, S. Saha, E. Suresh, A. Mandoli, R. Di Liddo, P. P. Parnigotto and A. Das, *Org. Lett*., 2010, **12**, 5406.
16 (a) X. Chen, X. Meng, S. Wang, Y. Cai, Y. Wu, Y. Feng, M. Zhu and Q. Guo, *Dalton Trans*., 2013, **42**, 14819; (b) Y. G. Zhao, Z. H. Lin, C. He, H. M. Wu and C. Y. Duan, *Inorg. Chem*., 2006, **45**, 10013; (c) M.-H. Yang, P. Thirupathi and K.-H. Lee, *Org. Lett*., 2011, **13**, 5028; (c) M. Santra, B. Roy and K. H. Ahn, *Org. Lett*., 2011, **13**, 3422.
17 (a) S. Sen, M. Mukherjee, K. Chakrabarty, I. Hauli, S. K. Mukhopadhyay and P. Chattopadhyay, *Org. Biomol. Chem.*, 2013, **11**, 1537; (b) L. E. Santos-Figueroa, M. E. Moragues, E. Climent, A. Agostini, R. Martínez-Mañez and F. Sancenon, *Chem. Soc. Rev.,* 2013, **42**, 3489.
18 (a) *Hydrogen Sulfide*; Geneva, World Health Organization, 1981 (Environmental Health Criteria, No. 19); (b) R. F. Huang, X. W. Zheng and Y. J. Qu, *Anal. Chim. Acta*, 2007, **582**, 267.
19 (a) R. E. Gosselin, R. P. Smith and H. C. Hodge, *Hydrogen Sulfide. In Clinical Toxicology of Commercial Products*, 5th ed.; Williams and Wilkins: Baltimore, MD, 1984; 198; (b) S. A. Patwardhan and S. M. Abhyankar, *Colourage*, 1988, **35**, 15.
20 (a) C. R. Liu, J. Pan, S. Li, Y. Zhao, L. Y. Wu, C. E. Berkman, A. R. Whorton and M. Xian, *Angew. Chem. Int. Ed*., 2011, **50**, 10327; (b) Y. J. Peng, J. Nanduri, G. Raghuraman, D. Souvannakitti, M. M. Gadalla, G. K. Kumar, S. H. Snyder and N. R. Prabhakar, *Proc. Natl. Acad. Sci. U.S.A.*, 2010, **107**, 10719; (c) Y. Kaneko, Y. Kimura, H. Kimura and I. Niki, *Diabetes*, 2006, **55**, 1391; (d) L. Li, M. Bhatia, Y. Z. Zhu, Y. C. Zhu, R. D. Ramnath, Z. J. Wang, F. B. M. Anuar, M. Whiteman, M. Salto-Tellez and P. K. Moore, *FASEB J.*, 2005, **19**, 1196; (e) K. Abe and H. *J.* Kimura, *Neurosci.*, 1996, **16**, 1066.

21 K. Eto, T. Asada, K. Arima, T. Makifuchi and H. Kimura, *Biochem. Biophys. Res. Commun*., 2002, **293**, 1485.

22 P. Kamoun, M. C. Belardinelli, A. Chabli, K. Lallouchi and B. Chadefaux-Vekemans, *Am. J. Med. Genet.*, 2003, **116**, 310.

23 W. Yang, G. Yang, X. Jia, L. Wu and R. Wang, *J. Physiol*., 2005, **569**, 519.

24 S. Fiorucci, E. Antonelli, A. Mencarelli, S. Orlandi, B. Renga, G. Rizzo, E. Distrutti, V. Shah and A. Morelli, *Hepatology*, 2005, **42**, 539.

25 (a) B. Valeur and I. Leray, *Coord. Chem. Rev.*, 2000, **205**, 3; (b) A. P. de Silva, H. Q. N. Gunaratne, T. Gunnlaugsson, A. J. M. Huxley, C. P. McCoy, J. T. Rademacher and T. E. Rice, *Chem. Rev.*, 1997, **97**, 1515; (c) Z. Xu, Y. Xiao, X. Qian, J. Cui and D. Cui, *Org. Lett.,* 2005, **7,** 889; (d) G. Grynkiewicz, M. Poenie and R. Y. Tsien, *J. Biol. Chem.*, 1985, **260**, 3440.

26 (a) X. F. Yang, X. Q. Guo and Y. B. Zhao, *Talanta*, 2002, ***57***, 883; (b) V. Dujols, F. Ford and A. W. Czarnik, *J. Am. Chem. Soc.*, 1997, **119**, 7386 .

27 X. Zhou, P. Li, Z. Shi, X. Tang, C. Chen and W. Liu, *Inorg Chem.*, 2012, **51**, 9226.

28 X. Zhang, Y. Xiao and X. Qian, *Angew. Chem. Int. Ed.*, 2008, **47**, 8025.

29 J. R. Lakowicz, *Principles of Fluorescence Spectroscopy*, Springer, 2006, 443.

30 G. M. Hale and M. R. Querry, *Appl. Opt.*, 1973, **12**, 555.

31 J. Ratha, K. A. Majumdar, S. K. Mandal, R. Bera, C. Sarkar, B. Saha, C. Mandal, K. D. Saha and R. Bhadra, *Mol. Cell Biochem*., 2006, **290**, 113.

32 (a) X. Chen, T. Pradhan, F. Wang, J. S. Kim and J. Yoon, *Chem. Rev.*, 2012, **112**, 1910; (b) M. Vendrell, D. Zhai, J. C. Er and Y. T. Chang, *Chem. Rev*., 2012, **112**, 4391; (c) C. Kar, M. D. Adhikari, A. Ramesh and G. Das, *Inorg. Chem.,* 2013, **52**, 743.

33 H. A. Benesi and J. H. Hildebrand, *J. Am. Chem. Soc*., 1949, **71**, 2703.

34 N. J. Turro, *Modern Molecular Photochemistry*, Benjamin/ Cummings Publishing Co., Inc. Menlo Park, CA, 1978.

35 J. A. Weyh and R. E. Hamm, *Inorg Chem.*, 1969, **8**, 2298.